

# Assessing the impact of a preprocessing stage on deep learning architectures for breast tumor multi-class classification with histopathological images

I. Calvo<sup>1</sup>, S. Calderon<sup>2</sup>, J. Torrents-Barrena<sup>3</sup>, E. Muñoz<sup>4</sup>, and D. Puig<sup>5</sup>

<sup>1,2,4</sup>Escuela de Computación, Tecnológico de Costa Rica, Costa Rica

<sup>3,5</sup>Dep. d'Enginyeria Informàtica i Matemàtiques, Universitat Rovira i Virgili, Spain

ivanfelipecp@gmail.com<sup>1</sup>, sacalderon@itcr.ac.cr<sup>2</sup>, jordina.torrents@urv.cat<sup>3</sup>,  
erickm968@gmail.com<sup>4</sup>, domenec.puig@urv.cat<sup>5</sup>

**Abstract.** In this work, we assess the impact of the adaptive unsharp mask filter as a preprocessing stage for breast tumour multi-class categorization with histopathological images, evaluating two state of the art architectures, not tested so far for this problem to our knowledge: DenseNet, SqueezeNet and a 5-layer baseline deep learning architecture. SqueezeNet is an efficient architecture, which can be useful in environments with restrictive computational resources. According to the results, the filter improved the accuracy from 2% to 4% in the 5-layer baseline architecture, on the other hand, DenseNet and SqueezeNet show a negative impact, losing from 2% to 6% accuracy. Hence, simpler deep learning architectures can take more advantage of filters than complex architectures, which are able to learn the preprocessing filter implemented. Squeeze net yielded the highest per parameter accuracy, while DenseNet achieved a 96% accuracy, defeating previous state of the art architectures by 1% to 5%, making Densenet a considerably more efficient architecture for breast tumour classification.

**Keywords:** Breast cancer · Histopathological images · Deep learning · Multi-class tumour classification

## 1 Introduction

Cancer is a major public health problem [3], it affects millions of people and every year, new cases and deaths are recorded globally. Breast cancer is the second most diagnosed cancer world-wide. Last year 2,088,849 new cases of breast cancer were discovered and 626,679 deaths registered [3].

Detecting and treating a tumour in early stages increases recovery and survival rates for patients. A method for estimating the stage and type of breast cancer is an histopathological image analysis, in which a pathologist examines an histology to diagnose an existing malign or benign tumour. Histopathological analysis is carried out after suspicious masses are found in a previous diagnostic mammogram.

Subjects with mammograms categorized by level 4 or 5 according the *Breast Imaging Reporting and Data System* (BI-RADS) standard, are usually advised to perform further histopathological analysis.

Based on the deep learning and architectures based on convolutional neural networks success for image analysis applications, the development of accurate *Computer Aided Diagnosis* (CAD) systems for medical purposes is becoming increasingly popular, however often limited by data availability from clinics and hospitals. Few initiatives for creating open data repositories can be found in the medical community. An example of these initiatives is the breast cancer histopathological database known as BreakHis [24]. This dataset is composed of breast tumor tissues images labeled as benign or malign.

Automated histopathological analysis systems can be implemented on a medic device or embedded system to support pathologist every day sample analysis, improving tumor detection accuracy, and allowing the pathologist to focus in most urgent cases. Moreover, efficient deep convolutional architectures are of interest for the usage in mobile phones and embedded computers. For small clinics in underdeveloped areas with poor internet access, implementing efficient deep learning architectures can be useful.

Frequently, data samples present noise or signal degradations, decreasing the signal to noise ratio. Therefore a preprocessing stage becomes necessary, with input images transformed, normalized, enhanced, denoised or filtered depending on the problem to solve. In [4, 5, 17, 20], different techniques are proposed for contrast enhancement and edge sharpening preprocessing.

In this work, we assessed the impact of an adaptive unsharp mask filter [17] as preprocessing stage for three different convolutional network architectures based approach for breast tumour multi classification, evaluating the breast cancer histopathological database(BreakHis) as training and testing data.

As contributions, we evaluated the intensity and edge based adaptive unsharp masking filter for color image enhancement as a preprocessing stage for breast tumour classification.

In order to evaluate the impact of a filter in complex and simpler architectures, we chose DenseNet and Squeezenet: two novel state of the art architectures. On the other hand, we also contribute to the state of the art on breast tumour classification, since to our knowledge, there is not a lot of related work with these two architectures on breast cancer multi-class classification problems.

## 2 State of the art

Deep learning has been a successful approach for the development of computer-aided systems for medical purposes, since its techniques, methods and architectures applied to medical images have yielded successful and accurate results so far [15, 19, 21, 22]. However, a challenge faced by the scientific community is the lack of open datasets to be able to develop and test these systems since most of the medical information is private. Recently, [24] authors and collaborators released a dataset of breast cancer histopathological images [24] for research and

benchmarking purposes, therefore, we focus our literature exploration in works presenting image analysis solutions tested with the BreakHis dataset. Binary classification is a common problem in computer vision and machine learning, in which the data is classified in two classes as BreakHis, that is divided in two mainly classes: benign and malign tumours.

In [2], authors present a study of the state of the art, as they compared their deep learning methods, the baseline model architecture(InceptionV3) and results with [23, 24, 25] for binary classification. In [24] authors used classical machine learning classification methods, meanwhile [25] used a standard convolutional neural network architecture and [23] an AlexNet model baseline [8]. [25] obtained the best results on patient level accuracy: 96.7%, 93.2%, 89.8%, 92.3% and 96.1%, 89.9%, 87.2%, 85.2% on image level accuracy in 40 $\times$ , 100 $\times$ , 200 $\times$  and 400 $\times$  magnifications respectively, on the other hand, [2] obtained the best results on F1 score: 93%, 88.9%, 89.4% and 86.4% in the respective magnifications.

Binary breast tumour classification is studied on [18], in this work, authors assess the impact of transfer learning on three pre-trained models: VGG16, VGG19, and ResNet50. All the models possess a logistic regression classifier as a top model. The fine-tuned pretrained VGG16 with logistic regression classifier yielded obtained the best performance with 92.60% accuracy.

Recent DenseNet architecture [13], based on the idea of implementing several skip connections to overcome the vanishing gradient problem, has been evaluated in [11] for breast tumour binary classification using the BreakHis dataset as training and testing data. Xgboost [6] was used for feature extraction and principal component analysis for dimensionality reduction. They achieved  $94.71 \pm 0.88$ ,  $95.9 \pm 4.2$ ,  $96.76 \pm 1.09$  and  $89.11 \pm 0.12$  in patient level accuracy on 40 $\times$ , 100 $\times$ , 200 $\times$  and 400 $\times$  magnifying factors respectively.

The two main classes of BreakHis: benign and malign are divided in four subtypes each, allowing to perform a multi-class classification to determine the type of tumour presented in a histology. Binary classification has been thoroughly investigated, [25] reports a maximum accuracy of 96%, therefore, we consider that binary classification on BreakHis is a solved and well-known problem through deep learning techniques, demonstrating a better performance and efficiency since feature extraction is learned through the training iterations by deep convolutional neural networks instead of handcrafted methods as [24], which employs traditional machine learning and feature extraction techniques to solve the binary classification, performing an accuracy of 73% to 85%. On the other hand, breast tumour multi-class classification is not solved and most of the authors in current literature address and face the multi-class breast tumour classification problem using deep convolutional networks, as is shown in [1], a deep learning convolutional neural network was evaluated and results of 91.54% accuracy have been reported on the BreakHis dataset.

Another approach is proposed in [12], which suggests an end-to-end recognition method by a novel deep learning based architecture to multi-class classification. A frequent problem in breast histopathological images is class imbalance, since samples for certain types of tumours are less common. To handle imbalanced

datasets as BreakHis, author used a data augmentation based approach and obtained an average of 93.2% accuracy.

Authors in [9] reported a 95.15% accuracy with a deep residual network based framework. The base model used is Resnet, which classifies between benign or malign, followed by a top meta decision tree that classifies the ResNet output between one of the different eight subtypes of tumours of the BreakHis dataset.

Preprocessing is an important stage on every deep learning baseline, in this step, data can be denoised or filtered depending on the problem to solve, in [4] authors analyze the impact of denoising, contrast and edge enhancement using the deceived non local means filter in a convolutional neural network based approach for age estimation using digital X-ray images from hands, this filter has two remarkable features: noise removing and border highlighting. Since the filter has two parameters, combinations were tested and reported the results for each. As conclusion, authors asserted the significance on how changing the parameters of the filter affects the learning process of the model. They proved that for some combinations, the filter improved the learning process and the accuracy of the deep learning model. This leads us to explore preprocessing impact in a deep learning classification model.

### 3 Proposed method

BreakHis dataset presents a wide variety of cases for the adaptive unsharp mask filter to be tested on, four magnification values, four types of benign and malign breast tumours. Since we aim to test the effect of the filter as a preprocessing stage, this assortment of scenarios allows us to test the behaviour of the AUM with images presenting different levels of detail and contrast. As seen in [4, 5] a filter can have a significant impact on the learning process and accuracy of a deep learning model.

The tested architectures deep learning DenseNet [13] and SqueezeNet [14]. We compare DenseNet since remarkable results have been reported in [10] on binary breast tumour classification.

We seek to assess the impact of the preprocessing stage has on a lightweight network a heavyweight one, this is why SqueezeNet and DenseNet are used. We know SqueezeNet is a lightweight network with a good number of parameters - accuracy ratio [14], and we aim to measure the impact of the proposed AUM preprocessing step, as also compare its accuracy and resource consumption with the more complex DenseNet architecture. DenseNet implements a lot of parameters, and is a huge network in comparison to SqueezeNet, thus we also test its multi classification accuracy. We want to measure the impact AUM has on of both big and small networks alike. All the architectures have a softmax function as a final activation for the eight prediction output, therefore, cross entropy was used as loss function.

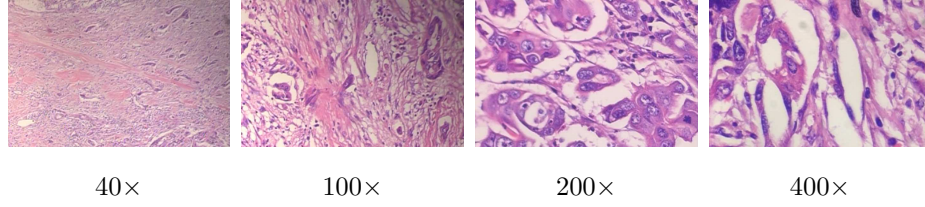
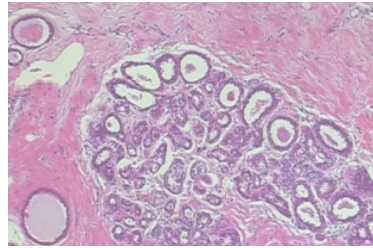


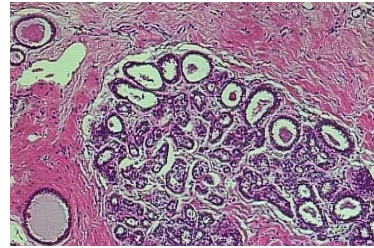
Fig. 1: Histopathological images from different magnifying factors.

### 3.1 Dataset

We evaluated the Breast Cancer Histopathological Database [24] known as BreakHis, composed of 7,909 microscopic images of breast tumor tissue collected from 82 patients using different magnifying factors (40 $\times$ , 100 $\times$ , 200 $\times$ , and 400 $\times$ ). The database is basically divided in two major classes: benign and malign. These two classes are then subdivided into four subtypes each: *Adenosis* (A), *Fibroadenoma* (F), *Phyllodes Tumour* (PT) and *Tubular Adenoma* (TA) as benign subtypes and *Carcinoma* (DC), *Lobular Carcinoma* (LC), *Mucinous Carcinoma* (MC) and *Papillary Carcinoma* (PC) as malignant subtypes.



(a) Pathological histology without AUM



(b) Pathological histology with AUM

Fig. 2: Original (a) and filtered (b) histopathological image from the BreakHis database.

### 3.2 Preprocessing: Adaptive Unsharp Mask

Previous work [4, 7] reported a significant performance impact of preprocessing on *Convolutional Neural Networks* (CNNs). Therefore, we used the intensity and edge based AUM filter [17] as a preprocessing stage. The filter enhances colorfulness via color channel stretching, and contrast by edge augmentation as is shown in figure. 2. The main difference in comparison with USM, is the iterative process in which the variable that controls the amount of image enhancement: gain factor, is determined and updated, unlike the USM filter that has a constant gain factor for all the pixels. This adaptive approach takes

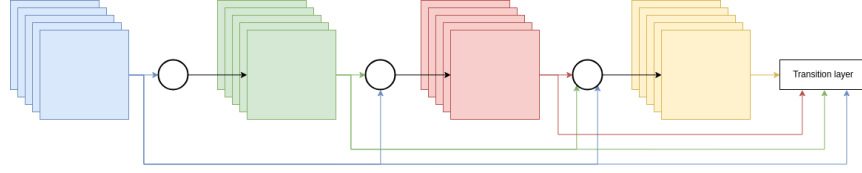


Fig. 3: Densed connectivity block

into account the global information of the image, obtaining better results on sharpness and contrast.

Once the AUM is applied, images are normalized from 0 to 1, and resized from  $700 \times 460$  to  $(n \times n)$  using bilinear interpolation to keep the image ratio, where  $n$  is the input size of the respective model.

### 3.3 DenseNet

The concept of a deep dense convolutional network known as DenseNet was proposed in [13]. The main goal of this architecture is to improve information and gradient flow between layers using dense connectivity blocks as is shown in figure 3. We evaluated the DenseNet 161-layer architecture who has 26,474,209 trainable parameters.

### 3.4 SqueezeNet

An important drawback of complex deep convolutional networks is usually the huge amount of parameters, which increases computational time and resources. To solve the aforementioned problem [14], the well-known SqueezeNet was proposed. It is an AlexNet-based architecture with 50x less parameters, lower size filters, downsampling and channel reduction.

The main feature of this architecture is the fire module. It is combined with convolution layers, another fire modules and max-pooling operations to create the SqueezeNet. A fire module relies on a compressing and expanding layer, the compressing layer has  $1 \times 1$  convolutional filters, which are then passed to the expanding layer composed of both  $1 \times 1$  and  $3 \times 3$  convolutional filters as is shown in figure 4. This model has 723,809 trainable parameters.

## 4 Experiments and results

We used a 5-fold cross-validation for training and testing. To divide the data we accounted for the number of images of each tumour sub type, in order to avoid class bias. To face class unbalance, the loss function was weighted and balanced according to the number of samples of each tumour class, forcing the model to punish more errors in classes with less samples.

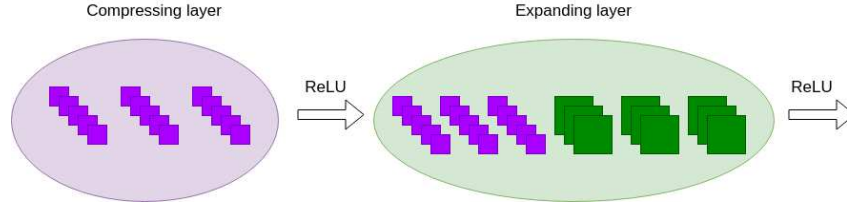


Fig. 4: Fire block

Each model was trained with 100 epochs; using Adam [16] optimizer with learning rate of 0.0001. The batch size used for training and testing was 28 and 18 for SqueezeNet and DenseNet, respectively, to avoid memory overflow.

To evaluate the performance of the models, we calculated the patient level accuracy, image level accuracy and F1-score.

The patient level accuracy metric is defined as follows. For each patient, let  $N_t$  be the total number of images and  $N_c$  the number of images correctly classified, then patient score  $S$  can be defined as:

$$S = \frac{N_c}{N_t} \quad (1)$$

Therefore, the patient level accuracy can be calculated as

$$\text{Patient level accuracy} = \frac{\sum_{i=1}^T S_i}{T} \quad (2)$$

Where  $T$  is the total number of patients.

The image level accuracy measures the rate of correctly classified images to the total number of images in the dataset. Let  $N$  be the total number of images in testing data and  $C$  the number of correctly classified images.

$$\text{Image level Accuracy} = \frac{C}{N} \quad (3)$$

DenseNet and SqueezeNet have obtained outstanding results [13, 14]. Therefore, we also evaluated a 5-layer deep CNN architecture, in order to evaluate the impact of preprocessing on a traditional deep convolutional baseline. The architecture is described in table 1, where  $b$  is the batch size.

Table 1: 5-layer CNN architecture

Layer	Input Size	Output Size	Kernel Size
Conv 1 + ReLU	(b,3,229,229)	(b,32,227,227)	3
Conv 2 + ReLU	(b,32,227,227)	(b,64,225,225)	3
Max pooling	(b,64,225,225)	(b,64,112,112)	2
BatchNorm	(b,64,112,112)	(b,64,112,112)	-
Conv 3 + ReLU	(b,64,112,112)	(b,128,110,110)	3
Conv 4 + ReLU	(b,128,110,110)	(b,256,108,108)	3
Max pooling	(b,256,108,108)	(b,256,54,54)	2
BatchNorm	(b,256,54,54)	(b,256,54,54)	-
Flat operation	(b,256,54,54)	(b,256*54*54)	-
FC + Softmax	(b,256*54*54)	(b,8)	-

Table 2: Patient level accuracy mean $\pm$ std

	Preprocessing		AUM	No AUM
	Architecture			
40 $\times$	DenseNet		0.94 $\pm$ .022	0.96 $\pm$ .013
	SqueezeNet		0.89 $\pm$ .027	0.95 $\pm$ .014
	5-layer CNN		0.45 $\pm$ .043	0.41 $\pm$ .057
100 $\times$	DenseNet		0.93 $\pm$ .018	0.93 $\pm$ .023
	SqueezeNet		0.89 $\pm$ .025	0.92 $\pm$ .021
	5-layer CNN		0.39 $\pm$ .026	0.38 $\pm$ .018
200 $\times$	DenseNet		0.91 $\pm$ .017	0.92 $\pm$ .016
	SqueezeNet		0.89 $\pm$ .012	0.88 $\pm$ .05
	5-layer CNN		0.48 $\pm$ .034	0.44 $\pm$ .023
400 $\times$	DenseNet		0.88 $\pm$ .025	0.9 $\pm$ .015
	SqueezeNet		0.79 $\pm$ .034	0.83 $\pm$ .069
	5-layer CNN		0.40 $\pm$ .039	0.39 $\pm$ .021

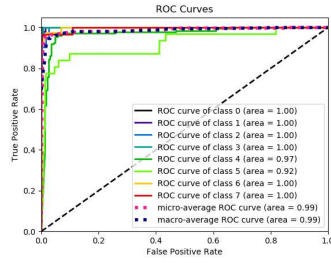
Table 3: Image level accuracy mean $\pm$ std

	Preprocessing		AUM	No AUM
	Architecture			
40 $\times$	DenseNet		0.95 $\pm$ .006	0.96 $\pm$ .012
	SqueezeNet		0.90 $\pm$ .015	0.94 $\pm$ .012
	5-layer CNN		0.53 $\pm$ .048	0.48 $\pm$ .038
100 $\times$	DenseNet		0.92 $\pm$ .013	0.94 $\pm$ .011
	SqueezeNet		0.88 $\pm$ .008	0.91 $\pm$ .013
	5-layer CNN		0.45 $\pm$ .015	0.45 $\pm$ .037
200 $\times$	DenseNet		0.90 $\pm$ .010	0.92 $\pm$ .015
	SqueezeNet		0.87 $\pm$ .009	0.89 $\pm$ .014
	5-layer CNN		0.51 $\pm$ .034	0.50 $\pm$ .016
400 $\times$	DenseNet		0.89 $\pm$ .013	0.91 $\pm$ .006
	SqueezeNet		0.80 $\pm$ .013	0.84 $\pm$ .019
	5-layer CNN		0.50 $\pm$ .017	0.46 $\pm$ .033

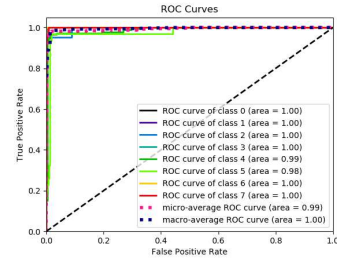


Table 4: F1-score mean $\pm$ std

Architecture	Preprocessing	AUM	No AUM
40 $\times$	DenseNet	0.94 $\pm$ .022	0.96 $\pm$ .035
	SqueezeNet	0.90 $\pm$ .051	0.94 $\pm$ .024
	5-layer CNN	0.61 $\pm$ .147	0.30 $\pm$ .143
100 $\times$	DenseNet	0.90 $\pm$ .034	0.93 $\pm$ .021
	SqueezeNet	0.87 $\pm$ .049	0.91 $\pm$ .037
	5-layer CNN	0.30 $\pm$ .110	0.27 $\pm$ .168
200 $\times$	DenseNet	0.89 $\pm$ .038	0.91 $\pm$ .042
	SqueezeNet	0.86 $\pm$ .053	0.88 $\pm$ .04
	5-layer CNN	0.37 $\pm$ .104	0.32 $\pm$ .067
400 $\times$	DenseNet	0.87 $\pm$ .061	0.90 $\pm$ .039
	SqueezeNet	0.78 $\pm$ .061	0.83 $\pm$ .057
	5-layer CNN	0.33 $\pm$ .118	0.32 $\pm$ .088

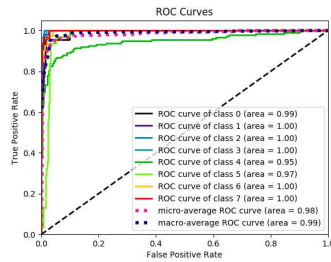


(a) AUM

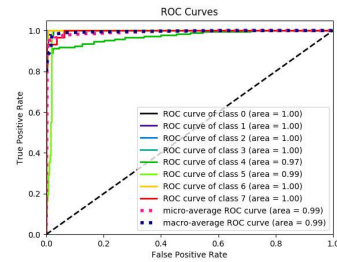


(b) No AUM

Fig. 5: ROC curve of DenseNet on x40 magnifying factor



(a) AUM



(b) No AUM

Fig. 6: ROC curve of SqueezeNet on x40 magnifying factor

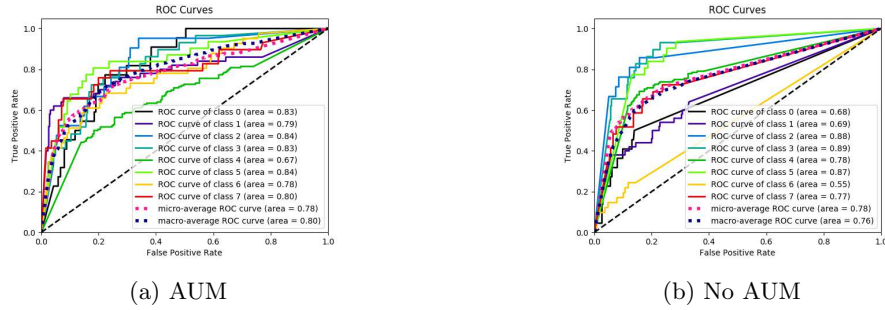


Fig. 7: ROC curve of 5-layer CNN on x40 magnifying factor

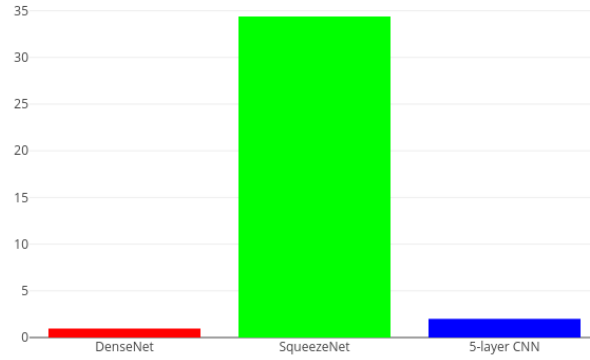


Fig. 8: Accuracy per parameter table scaled 0-100

Table 5: Comparison of 40 $\times$  magnifying factor results with other works, NR stands by non reported

Work	Patien level accuracy	Image level accuracy	F1-Score	Classification
[2]	91.5	90.2	93	Binary
[11]	NR	94.7	NR	Binary
[23]	84.0	84.6	88	Binary
[25]	90.0	85.6	92.9	Binary
[9]	NR	95.6	NR	Multi
[12]	94.1	92.8	NR	Multi
DenseNet with AUM	94.2	95.6	94.7	Multi
DenseNet without AUM	96.2	96.1	96.1	Multi
5-layer with AUM	45.5	53.4	47.3	Multi
5-layer without AUM	41.5	48.3	31.0	Multi

Looking at the F1-score in table 4 its clear that the preprocessing stage contributes in a negative manner, most of the cases for SqueezeNet and DenseNet, but in case of the 5-layer implementation it seems to improve the accuracy in some cases.

As previously discussed, the use of a adaptive unsharp mask preprocessing stage was proposed because an improvement in the accuracy of the model was expected, but results proved this supposition to be wrong. In tables 2 and 3 a considerable negative impact on patient and image level accuracy is seen on all implementations when using the *Adaptative Unsharpping Mask Filter* (AUM). DenseNet achieved 2% lower accuracy when using the AUM filter in it worse case, this can be due to it high amount of parameters that allow it to become numb to the changes made by the filter. On the other hand, the AUM had a larger negative impact on SqueezeNet, where the accuracy loss varies between 1% and 6% using 200x and 40x magnification respectively, it can be argued that this is because of network having less parameters and therefore less flexibility to adjust the change produced by the filter.

As for the 5-layer CNN tested, it yielded an important accuracy increase when using the AUM as a preprocessing stage, yielding an accuracy boost of around 5%, as seen in tables 2 and 3. The lack of generalization can be appreciated in figure 7, which shows the positive ratio of 5-layer CNN model trained with and without AUM. The *Receiver Operating Characteristics* (ROC) curve shows a better positive ratio by the AUM model, showing a better percentage of true positives in comparison to the model without AUM that focus on classes 2 (F), 3 (PT) and 4 (TA). Contrary case is observed in DenseNet and SqueezeNet ROC curves on figures 5 and 6, where the positive ratio with and without AUM is alike.

When using the F1 score to measure the accuracy for each class in the dataset, a clear pattern can be seen in table 5, that is the negative effect the AUM has on elaborate networks like DenseNet and SqueezeNet. It seems like the use of the filter might even removing information useful in the classification process, this effect was not present when the 5-layer CNN was tested, instead an significant improvement of almost 30% was achieved in some cases and in others a downgrade was also reported.

According to the results obtained, DenseNet achieved the highest (96%) F1-score, patient and image level accuracy. Both architectures DenseNet and SqueezeNet demonstrated an important decrease in precision. On the contrary, simpler models (e.g., 5-layer CNN) provided a significant performance gain with AUM images. Therefore, very basic CNNs can take more advantage of preprocessing than complex state-of-the-art architectures. Note that similar results and conclusions were previously obtained in [5].

The top performance of each model is obtained in 40 $\times$  magnifying factor since the images posses global information that is removed when the magnifying factor increases, affecting the learning of the models. Thus, table 5 reports the results with other works on this specific magnifying factor, showing that DenseNet obtained a better performance than other works. It can be noted that as the

input image has a higher magnifiers factor, the accuracy decreases, this happens not only on DenseNet but all tested architectures. This could be due the fact that as the magnification increases the amount of local information captured in each image is less, and it ends up being a very localized picture, therefore losing important information of the surrounding area.

Moreover, SqueezeNet ranked second using less than 25 million parameters compared to DenseNet. Although it is fast, there is room for improvement regarding accuracy rates. SqueezeNet is also a lightweight network that offers a remarkable efficiency per parameter. This feature could be useful in a embedded environment as a first line of detection in an histology, and become, to our knowledge, the first neural network to be used in a embedded system for breast tumour detection. The considerable resource consumption/accuracy higher ratio of SqueezeNet can be seen in figure 8.

## 5 Conclusions

We analyzed the impact of the preprocessing AUM filter on three different deep learning architectures to classify breast tumours in histopathological images and determined that the usage of this preprocessing stage for DenseNet and SqueezeNet decreases the accuracy of both networks in every single test case, with variable magnification and multiple classes. It can be said that the filter removes key characteristics from the images and this does not help with the learning process of this networks, as also more complex networks are likely to become numb to noisy or degraded samples. On the other hand the 5-layer CNN architecture improved its results and showed that simple convolutional architectures can be enhanced by the use if this kind of preprocessing stage for histopathological images, as it is less likely to learn the filter behavior by itself.

The results obtained by DenseNet and SqueezeNet shows the negative impact of the filter on complex architectures in comparison with the 5-layer CNN, whose results improved significantly with the filter, meaning that small and simpler convolutional neural networks can take more advantage and benefits of filters than complex architectures.

SqueezeNet yielded an outstanding accuracy per parameter, demonstrating that huge amount of parameters are not necessary to achieve a satisfactory accuracy. Is also a suitable architecture to be used in medical devices or embedded system as an extra help to help detect cases higher risk of developing cancer, being specially useful in places were there are many cases to check but very few people to do the job. SqueezeNet proved to be a potentially viable network to be used in embedded systems due to its low parameter but high accuracy relation, it showed it's capable of being toe to toe with a network as huge as DenseNet.

## Bibliography

- [1] Adeshina, S.A., Adedigba, A.P., Adeniyi, A.A., Aibinu, A.M.: Breast cancer histopathology image classification with deep convolutional neural networks. In: 2018 14th International Conference on Electronics Computer and Computation (ICECCO). pp. 206–212. IEEE (2018)
- [2] Benhammou, Y., Tabik, S., Achchab, B., Herrera, F.: A first study exploring the performance of the state-of-the art cnn model in the problem of breast cancer. In: Proceedings of the International Conference on Learning and Optimization Algorithms: Theory and Applications. p. 47. ACM (2018)
- [3] Bray, F., Ferlay, J., Soerjomataram, I., Siegel, R.L., Torre, L.A., Jemal, A.: Global cancer statistics 2018: Globocan estimates of incidence and mortality worldwide for 36 cancers in 185 countries. *CA: a cancer journal for clinicians* **68**(6), 394–424 (2018)
- [4] Calderon, S., Fallas, F., Zumbado, M., Tyrrell, P., Stark, H., Emersic, Z., Meden, B., Solis, M.: Assessing the impact of the deceived non local means filter as a preprocessing stage in a convolutional neural network based approach for age estimation using digital hand x-ray images. In: 2018 25th IEEE International Conference on Image Processing (ICIP). pp. 1752–1756. IEEE (2018)
- [5] Carranza, J., S.Calderon, A.Mora-Fallas, M.Granados-Menani: Unsharp masking layer: Injecting prior knowledge in convolutional networks for image classification, in press
- [6] Chen, T., Guestrin, C.: Xgboost: A scalable tree boosting system. In: Proceedings of the 22nd acm sigkdd international conference on knowledge discovery and data mining. pp. 785–794. ACM (2016)
- [7] Dodge, S., Karam, L.: Understanding how image quality affects deep neural networks. In: 2016 eighth international conference on quality of multimedia experience (QoMEX). pp. 1–6. IEEE (2016)
- [8] Donahue, J., Jia, Y., Vinyals, O., Hoffman, J., Zhang, N., Tzeng, E., Darrell, T.: Decaf: A deep convolutional activation feature for generic visual recognition. In: International conference on machine learning. pp. 647–655 (2014)
- [9] Gandomkar, Z., Brennan, P.C., Mello-Thoms, C.: Mudern: Multi-category classification of breast histopathological image using deep residual networks. *Artificial intelligence in medicine* **88**, 14–24 (2018)
- [10] Gu, Y., Jie, Y.: Densely-connected multi-magnification hashing for histopathological image retrieval. *IEEE journal of biomedical and health informatics* (2018)
- [11] Gupta, V., Bhavsar, A.: Sequential modeling of deep features for breast cancer histopathological image classification. In: Proceedings of the IEEE Conference on Computer Vision and Pattern Recognition Workshops. pp. 2254–2261 (2018)

- [12] Han, Z., Wei, B., Zheng, Y., Yin, Y., Li, K., Li, S.: Breast cancer multi-classification from histopathological images with structured deep learning model. *Scientific reports* **7**(1), 4172 (2017)
- [13] Huang, G., Liu, Z., Van Der Maaten, L., Weinberger, K.Q.: Densely connected convolutional networks. In: *Proceedings of the IEEE conference on computer vision and pattern recognition*. pp. 4700–4708 (2017)
- [14] Iandola, F.N., Han, S., Moskewicz, M.W., Ashraf, K., Dally, W.J., Keutzer, K.: Squeezenet: Alexnet-level accuracy with 50x fewer parameters and 0.5 mb model size. *arXiv preprint arXiv:1602.07360* (2016)
- [15] Khosravan, N., Celik, H., Turkbey, B., Jones, E.C., Wood, B., Bagci, U.: A collaborative computer aided diagnosis (c-cad) system with eye-tracking, sparse attentional model, and deep learning. *Medical image analysis* **51**, 101–115 (2019)
- [16] Kingma, D.P., Ba, J.: Adam: A method for stochastic optimization. *arXiv preprint arXiv:1412.6980* (2014)
- [17] Lin, S., Wong, C., Jiang, G., Rahman, M., Ren, T., Kwok, N., Shi, H., Yu, Y.H., Wu, T.: Intensity and edge based adaptive unsharp masking filter for color image enhancement. *Optik* **127**(1), 407–414 (2016)
- [18] Mehra, R., et al.: Breast cancer histology images classification: Training from scratch or transfer learning? *ICT Express* **4**(4), 247–254 (2018)
- [19] Pertuz, S., Julia, C., Puig, D.: A novel mammography image representation framework with application to image registration. In: *2014 22nd International Conference on Pattern Recognition*. pp. 3292–3297. IEEE (2014)
- [20] Polesel, A., Ramponi, G., Mathews, V.J.: Image enhancement via adaptive unsharp masking. *IEEE transactions on image processing* **9**(3), 505–510 (2000)
- [21] Shin, H.C., Roth, H.R., Gao, M., Lu, L., Xu, Z., Nogues, I., Yao, J., Mollura, D., Summers, R.M.: Deep convolutional neural networks for computer-aided detection: Cnn architectures, dataset characteristics and transfer learning. *IEEE transactions on medical imaging* **35**(5), 1285–1298 (2016)
- [22] Singh, V.K., Romani, S., Rashwan, H.A., Akram, F., Pandey, N., Sarker, M.M.K., Abdulwahab, S., Torrents-Barrena, J., Saleh, A., Arquez, M., et al.: Conditional generative adversarial and convolutional networks for x-ray breast mass segmentation and shape classification. In: *International Conference on Medical Image Computing and Computer-Assisted Intervention*. pp. 833–840. Springer (2018)
- [23] Spanhol, F.A., Oliveira, L.S., Cavalin, P.R., Petitjean, C., Heutte, L.: Deep features for breast cancer histopathological image classification. In: *2017 IEEE International Conference on Systems, Man, and Cybernetics (SMC)*. pp. 1868–1873. IEEE (2017)
- [24] Spanhol, F.A., Oliveira, L.S., Petitjean, C., Heutte, L.: A dataset for breast cancer histopathological image classification. *IEEE Transactions on Biomedical Engineering* **63**(7), 1455–1462 (2016)
- [25] Spanhol, F.A., Oliveira, L.S., Petitjean, C., Heutte, L.: Breast cancer histopathological image classification using convolutional neural networks. In: *2016 International Joint Conference on Neural Networks (IJCNN)*. pp. 2560–2567. IEEE (2016)